Comparison of the Photocatalytic Degradation of Congo Red Dye Using NiO and NiO-NiFe2O4 Composite

by Poedji Loekitowati

Comparison of the Photocatalytic Degradation of Congo Red Dye Using NiO and NiO-NiFe$_2$O$_4$ Composite

Poedji Loekitowati Hariani, Muhammad Said, Addy Rachmat, Astri Nurmansyah, and Ra Hoetary Tirta Amallia

Abstract—NiO and NiO-NiFe$_2$O$_4$, composite had been synthesized by the coprecipitation method and characterized using XRD, FTIR, UV-DRS, and SEM-EDS. The photocatalytic degradation performances of the photocatalyst were investigated using visible irradiation, in which Congo red dye was used as a model. The photocatalytic degradation process was assessed through three variables: the pH of the solution, Congo red dye initial concentration, and irradiation time. The removal efficiency of photocatalytic degradation of 98.45% was achieved using NiO-NiFe$_2$O$_4$ at a pH of 6, an initial concentration of the dye of 100 mg/L, and an irradiation time of 120 minutes is higher than that obtained using NiO, which was 78.5%. Pseudo-first-order was suitable to describe the kinetics of photocatalytic degradation of Congo red, with values of k = 0.0114 min^{-1} and t$_{1/2}$ = 60.789 min using NiO as the photocatalyst, and with k =0.0225 min^{-1} and t$_{1/2}$= 30.8 min using NiO-NiFe$_2$O$_4$. The removal efficiency of the NiO-NiFe$_2$O$_4$ composite of consecutive reuse three-time was 98.45, 97.13, and 96.21%, while NiO was 78.30, 77.12, and 75.32%. Therefore, NiO-NiFe$_2$O$_4$ was considered more effective in reducing Congo red concentration than NiO.

Index Terms—NiO, NiO-NiFe$_2$O$_4$ composite, photocatalytic, degradation, Congo red.

I. INTRODUCTION

Many environmental problems have emerged due to human activities. Water pollution is one of the problems that can cause physical, chemical, and biological changes in natural water. Such pollution does not affect aquatic ecosystems only but also living things [1]. Industrialization plays a role in water pollution. The textile, paper, soap, plastic, paint, food, and petrochemical industries produce waste in the form of dyes [2]. About 15-50% of dyes used in the textile industry are not bound to the fabric, thus discharged as liquid waste [3].

Heterogeneous photocatalysis is considered a destructive technology that leads to the mineralization of organic compounds, in which the degradation of compounds occurs in water by the action of a semiconductor material illuminated by light. Semiconductor oxides such as TiO$_2$ [4], ZnO [5], SnO$_2$ [6], NiO [7], and others are reported as photocatalysts for the degradation of organic pollutants.

p-type semiconductor metal oxides, such as NiO, are used as photocatalysts. NiO is chemically stable, it has low-cost synthesis and low toxicity, and exhibits remarkable electro-optic capabilities with a wide bandgap between the valence and conduction bands (3.2–4.0 eV), making it suitable to be a photocatalyst [1], [8]. NiO has been used in the degradation of organic dyes such as Rhodamine B [9], Methylene blue [10], and methyl orange [11].

Spinel ferrite compounds (MFe$_2$O$_4$; M = Fe, Co, Ni, Mn, Zn, and others) have been attracting much attention because of their wide practical applications in various fields as catalysts [12] and magnetic adsorbents [13], as well as for magnetic resonance imaging [14]. Nickel ferrite (NiFe$_2$O$_4$) is one of the most important spinel ferrite compounds for its excellent properties: high saturation magnetization and a unique magnetic structure [15].

One of the main problems in heterogeneous photocatalysis the wide band gap and electron-hole pair recombination, which significantly lower the photocatalytic efficiency [16], [17]. This problem can be relatively solved by doping, supporting, and coupling the semiconductor with other materials. In the hetero-junction system, the electron-hole recombination is significantly reduced. Thus, increasing the photodegradation efficiency.

Spinel ferrite compound has a band gap of about 2 eV [18], thus able to enhance the photocatalytic effect of NiO in the visible region. NiFe$_2$O$_4$ has moderate saturation magnetization, strong catalytic properties, photochemical stability, and high adsorption [19]-[22]. Magnetic properties provide an advantage because, after the degradation process, the photocatalyst can separate quickly using permanent magnets. Several researchers reported studies of photocatalysis of ferrites and metal oxides such as CuFe$_2$O$_4$-Ag$_2$O and CuFe$_2$O$_4$-NiO [23], TiO$_2$-NiFe$_2$O$_4$ [24], ZnO-CoFe$_2$O$_4$ [25], NiFe$_2$O$_4$-ZnO [26].

Several methods are applicable for the synthesis of NiO and NiO-NiFe$_2$O$_4$ such as the sol-gel [8], microwave and hydrothermal route [27], thermal decomposition [7], and coprecipitation [11]. In this study, the synthesis of NiO and NiO-NiFe$_2$O$_4$ composite was performed using the coprecipitation method. The method is simple and has a high product yield. Furthermore, the photocatalytic activities of NiO and NiO-NiFe$_2$O$_4$ composite were compared against Congo red dye using visible irradiation. Congo red dye is an anionic dye that is an issue for health [28]. Both NiO and NiO-NiFe$_2$O$_4$ were characterized using XRD, FTIR, SEM-EDS, and UV DRS.

II. EXPERIMENTAL

A. Materials

The chemicals used were $Ni(NO_3)_3 \cdot 6H_2O$, $Fe(NO_3)_3 \cdot 9H_2O$, NaOH, $NiSO_4 \cdot 6H_2O$, NaCl, HCl, and Congo red produced by Merck, Germany.

B. Synthesis of $NiFe_2O_4$

A total of 2.91 g of $Ni(NO_3)_3 \cdot 6H_2O$ and 8.08 g of $Fe(NO_3)_3 \cdot 9H_2O$ were dissolved in 100 mL of distilled water. NaOH was added slowly to the mixture while stirred by a magnetic stirrer until the pH of the solution reached 10. The precipitate formed was washed using distilled water and then dried in an oven for 1 hour at 100 °C, and then calcined using a furnace at a temperature of 800 °C for 2 hours.

C. Synthesis of NiO

A total of 3.09 g of $NiSO_4 \cdot 6H_2O$ was dissolved in 100 mL of distilled water. 1 M NaOH was added slowly into the solution until reaching a pH of 10 while stirred using a magnetic stirrer. The precipitate formed was separated and washed using distilled water, then dried using an oven for 1 hour at 100 °C, and calcined in a furnace at a temperature of 600°C for 2 hours.

D. Synthesis of NiO-$NiFe_2O_4$ Composite

The synthesis of NiO-$NiFe_2O_4$ composite with a weight ratio of 3:1 was carried out by adding 0.5 g of $NiFe_2O_4$ to 50 mL of 0.01 moL $NiSO_4 \cdot 6H_2O$. 1 M NaOH solution was added slowly into the mixture until the solution reached a pH of 10 using a magnetic stirrer. Drying was carried out in an oven for 1 hour at a temperature of 100°C. The precipitate was calcined in a furnace at a temperature of 600°C for 2 hours.

E. Characterization of NiO dan NiO-$NiFe_2O_4$

X-ray diffraction method (Rigaku Miniflex-600) was used to determine the crystal structure. The product functional group was determined using Fourier transform infrared (Prestige 21 Shimadzu) at a wavenumber region of 400-4000 cm^{-1}. The morphology and elemental composition of the product were determined using Scanning electron microscopy/energy-dispersive X-ray spectroscopy (SEM-EDS JSM 6510). The absorbance spectrum of the product was observed using UV–vis diffuse reflectance spectroscopy (Pharmaspec UV-1700).

The pHpzc of the product was determined in the following way. As much as 50 mL of a 0.01 M NaCl solution, having a pH adjusted to 2-12 using 0.1 M HCl or NaOH, was put into conical flasks containing 0.1 g of NiO and NiO-$NiFe_2O_4$ composite. The mixture was stirred for 24 hours using a shaker. Both the initial and final pH levels were determined using a pH meter. pHpzc was obtained from the graph of initial pH versus ΔpH [29].

F. Photocatalytic Degradation of Congo Red

The experiment at room temperature in a closed reactor using 5 Vis-LED irradiation lamps (15 W). Stirring was done using a magnetic stirrer. Observation of the effect of pH on the photocatalytic degradation process used Congo red solution with a concentration of 100 mg/L as much as 50 mL, a photocatalyst weight of 0.05 g, and an irradiation duration of 120 minutes. The pH in the range 2-9 was regulated using HCl or 0.1 M NaOH. The effect of the initial concentration of Congo red dye was observed in the range of 50-400 mg/L and the duration of irradiation ranging from 20-160 minutes. Congo red dye concentration in the solution was determined using a UV-Vis spectrophotometer (Genesys 10S). Removal Efficiency (RE) was determined based on the formula:

$$RE\ (\%) = \frac{C_0 - C_t}{C_0} \times 100$$

in which C_0 and C_t are the initial and instantaneous concentrations of Congo red (mg/L).

III. RESULT AND DISCUSSION

A. NiO and NiO-$NiFe_2O_4$ Composite Characterization

Fig. 1 shows the diffraction peaks of NiO and NiO-$NiFe_2O_4$. NiO has a crystalline structure with a cubic phase where the main peaks of NiO can be identified at 2θ = 37.37° (111), 43.6° (200), 62.6° (220), 76.1° (311) dan 79.7° (222), according to JCPDS N0 78- 0423. High intensity and broad spectra indicate the absence of impurities and high crystallinity. The calculation results on the crystal size of NiO using the Scherrer equation obtained an average crystal size of 7.6 nm. With the same method but at different calcination temperatures (700 and 750 °C), NiO was obtained to have about 6 nm [9], while at 400°C, it was about 8.06 nm [27].

Meanwhile, NiO-$NiFe_2O_4$ composite peaks show lower intensity than NiO. Some 2θ angles as the main characteristics of $NiFe_2O_4$ appear at 35.71° (311), 43.41° (400), and 63.1° (440). The appearance of these peaks proved the success of the synthesis of the composite. The crystal size of the NiO-$NiFe_2O_4$ composite was 10.2 nm/23.4 nm.
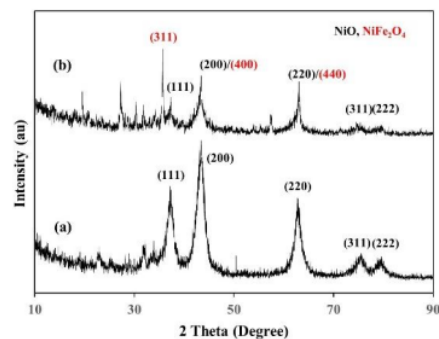

Fig. 1. XRD spectra of (a) NiO and (b) NiO-$NiFe_2O_4$ composite.

The FTIR spectra of NiO and the composite NiO-$NiFe_2O_4$ are present in Fig. 2. The spectra have similar wavenumbers but different peak sharpness. The broad peak in the wavenumber region of 3200-3500 cm^{-1} confirms the presence of O-H stretching vibration, while that at around 1624 cm^{-1} indicates the H-O-H bending vibration from the absorption of water molecules [30]. The wavenumber region at 400-700 cm^{-1} shows metal-oxygen stretching vibration, namely of Fe-O and Ni-O.

The morphology of NiO and NiO-$NiFe_2O_4$ composite is shown in Fig. 3. The surface of NiO appears not homogeneous, different both shape and size, tend to

agglomerate, while that of the composite NiO-NiFe$_2$O$_4$ appears denser. Table I shows the elements contained in NiO and NiO-NiFe$_2$O$_4$ composite based on the analysis using EDS. NiO is composed of Ni and O elements, while NiO-NiFe$_2$O$_4$ composite has an additional of Fe (36.4 %). EDS results also showed that no other elements were found, either in NiO or NiO-NiFe$_2$O$_4$ composite, thus indicating the purity of the synthesized material.
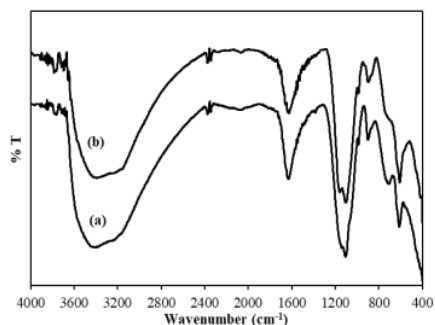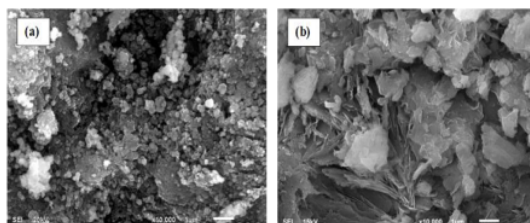

Fig. 2. FTIR spectra of (a) NiO and (b) NiO-NiFe$_2$O$_4$ composite.

Fig. 3. SEM image of (a) NiO and (b) NiO-NiFe$_2$O$_4$ composite.

TABLE I: THE ELEMENT COMPOSITION

Photocatalyst	Ni (%)	O (%)	Fe (%)
NiO	76.4	23.6	-
NiO-NiFe$_2$O$_4$	38.8	24.8	36.4

Bandgap value is a significant parameter for photocatalytic semiconductor materials [8]. A semiconductor's bandgap value can affect its performance in the excitation of electrons from the valence band to the conduction band that then undergo de-excitation, depending on the width of the energy gap generated by the semiconductor. NiO has a band gap > 3.0 eV. The band gap value depends on the synthesis method used, such as the band gap of NiO synthesized by the nebulizer spray pyrolysis method, namely 3.67 eV [31] and the bandgaps of NiO synthesized by the microwave and hydrothermal method of 3.2 and 3.5 eV, respectively [27].

In this study, the band gap of NiO was found to be 3.3 eV. The addition of NiFe$_2$O$_4$ causes a decrease in the band gap value, which is 2.8 eV. Spinel ferrite compounds have a band gap of about 2 eV, the band gap of NiFe$_2$O$_4$ synthesized by the solution combustion method was obtained at 1.97 eV [18], [32]. The presence of NiFe$_2$O$_4$ can cause a significant absorption shift to the visible light region compared to pure photocatalysts. Figs. 4 and 5 show the optical absorption and band gap values of NiO and NiO-NiFe$_2$O$_4$ composite. NiO has the largest absorbance at a wavelength of 362 nm, while NiO-NiFe$_2$O$_4$ composite has a larger wavelength of 410 nm. The addition of NiFe$_2$O$_4$ shifts the wavelength of maximum absorption.
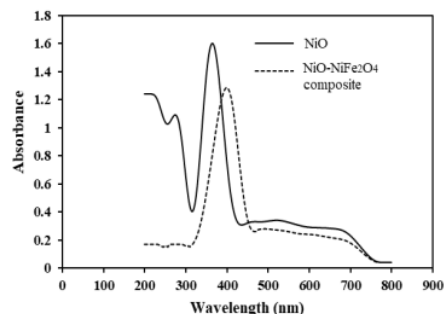

Fig. 4. Spectra UV-Vis DRS of NiO and NiO-NiFe$_2$O$_4$ composite.
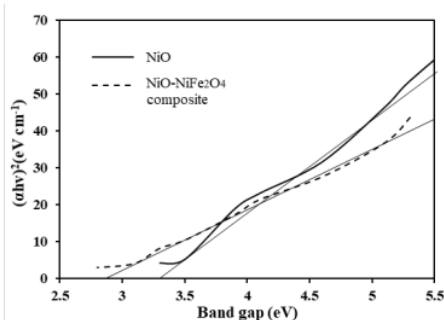

Fig. 5. Band gaps of NiO and NiO-NiFe$_2$O$_4$ composite.

B. Photocatalytic Degradation

In this study, the photocatalytic degradation of dye was carried out in various conditions, namely the pH of the solution, the initial concentration of the dye, and the irradiation duration. The pH of the solution is an important factor in the photocatalytic degradation process. Figs. 6 and 7 show the pHpzc of photocatalyst and the effect of solution pH on removal efficiency. The optimum pH for photocatalytic degradation of Congo red was obtained at a pH of 6 using the photocatalyst NiO and the composite NiO-NiFe$_2$O$_4$.

Congo red dye is anionic with two sulfonate groups; photocatalytic effectiveness is more effectively carried out at a pH below the pHpzc of the catalyst. The pHpzc values of NiO and NiO-NiFe$_2$O$_4$ composite were 6.3 and 6.6, respectively. At pH <pHpzc, the photocatalyst is positively charged, and the dye is negatively charged. The attraction of these different charges increases the effectiveness of photocatalytic degradation. The removal efficiency of NiO-NiFe$_2$O$_4$ composite is more than NiO because NiFe$_2$O$_4$ itself was also photocatalytic [32].
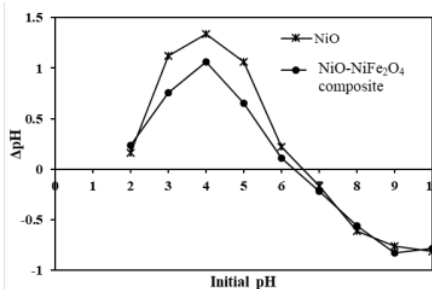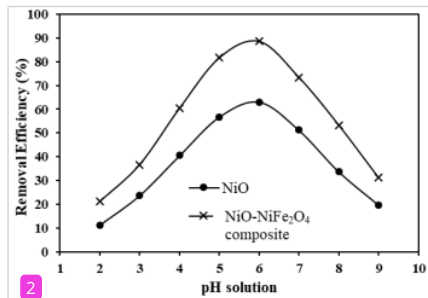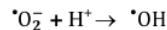

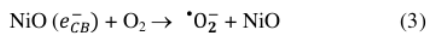Fig. 6. pHpzc values of NiO and NiO-NiFe$_2$O$_4$ composite.

Fig. 7. Photocatalytic Degradation of Congo red dye by variation of pH solution.

The degradation mechanism is that $NiFe_2O_4$ undergoes photoexcitation because it has a narrow bandgap, then electrons are photogenerated to the conduction band of NiO. The reaction is described as follows [7], [27]:

$$NiFe_2O_4 + h_v \rightarrow NiFe_2O_4\ (e_{CB}^- + h_{VB}^+) \qquad (1)$$

$$NiFe_2O_4\ (e_{CB}^-) + NiO \rightarrow NiFe_2O_4 + NiO(e_{CB}^-) \qquad (2)$$

$$NiO\ (e_{CB}^-) + O_2 \rightarrow {}^\bullet O_2^- + NiO \qquad (3)$$

$${}^\bullet O_2^- + H^+ \rightarrow {}^\bullet OH \qquad$$

The reaction of holes h_{VB}^+ and H_2O or OH^- produces ${}^\bullet OH$.

$$h_{VB}^+ + H_2O \rightarrow {}^\bullet OH + H^+ \qquad (4)$$

$$h_{VB}^+ + OH^- \rightarrow {}^\bullet OH \qquad (5)$$

$$CR + (h_{VB}^+ + {}^\bullet O_2^- + {}^\bullet OH) \rightarrow NiO + H_2O \qquad (6)$$

The surface of Congo red dye was attacked by h_{VB}^+ and ${}^\bullet O_2^- + {}^\bullet OH$, causing bond breaking and decolorization. The effect of dye concentration on the removal efficiency of the photocatalytic degradation of Congo red dye is present in Fig. 8. Photocatalytic degradation was carried out at a pH of 6 with an irradiation time of 120 minutes. The greater the concentration, the lower the removal efficiency. The photocatalytic degradation process rapidly at low concentrations. At high concentrations, the dye blocks radiation, causing only a small amount of radiation to reach the catalyst, thus reducing the number of radicals that play a role in the degradation process.
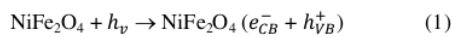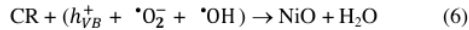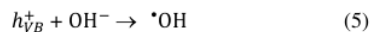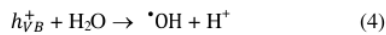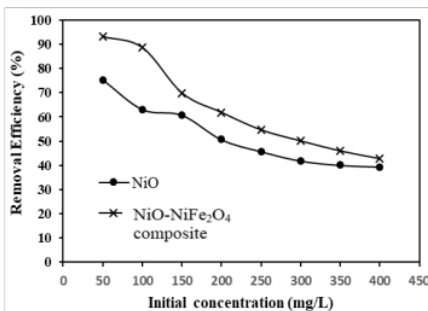

Fig. 8. Photocatalytic degradation of Congo red dye by variation of initial concentration.

Fig. 9 shows the effect of irradiation duration on the removal efficiency of photocatalytic degradation of Congo red dye using visible and non-irradiated light irradiation. The photocatalytic degradation process was carried out with the initial concentration of Congo red dye 50 mg/L at a pH solution of 6. There was a significant difference between using radiation and without it; removal efficiency without radiation is less than 10%. The longer the radiation process, the more Congo red dye degrades using both catalysts NiO and $NiO-NiFe_2O_4$ composite. The longer the radiation time, the more radicals produced react with the dye. Removal efficiency degradation using the catalyst of NiO was 78.5%, while that using $NiO-NiFe_2O_4$ composite was 98.45 %.
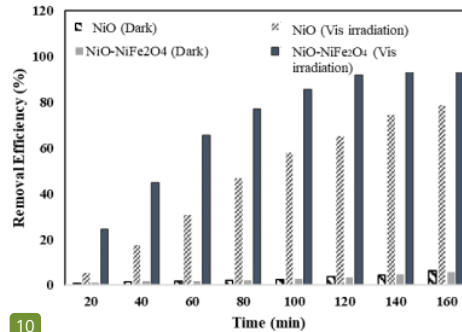
Fig. 9. Photocatalytic degradation of Congo red dye by variation of irradiation time.

C. Kinetics of Photocatalytic Degradation

Photocatalytic degradation of Congo red dye using NiO and $NiO-NiFe_2O_4$ composite is presented in Fig. 10. Kinetics of photocatalytic degradation was investigated using the equation [33]:

$$\ln C_0/C_t = k\ t$$

The linearity of $\ln C_0 / C_t$ versus t (time) shows pseudo-first-order. Table 2 shows the parameter pseudo-first-order kinetics for photocatalytic degradation of Congo red. The correlation coefficient value (R^2) using NiO and the $NiO-NiFe_2O_4$ composite is close to 1. The k value is calculated from the slope. The k value of the $NiO-NiFe_2O_4$ composite (0.0225 min^{-1}) was higher than that of NiO (0.0114 min^{-1}), indicating that the addition of $NiFe_2O_4$ increased the efficiency of photocatalytic degradation. the $t_{1/2}$ value = 0.693/k is shown in Table II.

Fig. 10. Pseudo-first-order kinetics for photocatalytic degradation.

TABLE II: THE PARAMETER PSEUDO-FIRST-ORDER

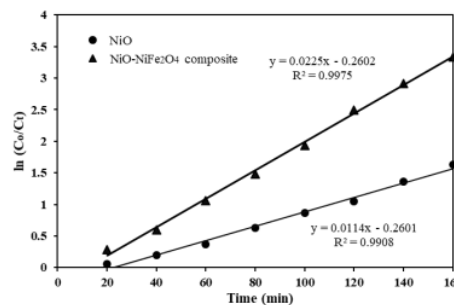| Materials	k (min^{-1})	t$_{1/2}$ (min)	R^2
NiO	0.0114	60.789	0.9908
NiO-NiFe$_2$O$_4$	0.0225	30.800	0.9975

Table III shows several photocatalytic degradation processes for Congo red dye using several catalysts. The removal efficiency of photocatalytic degradation of Congo red dye using the composite NiO-NiFe$_2$O$_4$ in this study was greater than previously reported by other researchers.

TABLE III: COMPARISON OF PHOTOCALITYC DEGRADATION WITH DIFFERENT MATERIALS

Photo catalyst	CR (mg/L)	Time (h)	Dosis (g/L)	Irr. Source	Rem. (%)	Ref.
NiFe$_2$O$_4$	100	1	0.5	Visible	96.8	[32]
CoFe$_2$O$_4$	5	1.5	0.35	UV	91	[34]
TiO$_2$	55	8	1	UV	20	[35]
NiFe$_2$O$_4$/ ZnO	20	0.16	1	Solar light	94.55	[26]
Mg-TiO$_2$- P25	7	7	0.5	Visible	80	[36]
NiO	50	2	1	Visible	78.5	This study
NiO-NiFe$_2$O$_4$	50	2.6	1	Visible	98.45	This study

D. Reusability of NiO and NiO-NiFe$_2$O$_4$ composite

The stability and efficiency of the catalyst in repeated use determine its reusability. NiO and NiO-NiFe$_2$O$_4$ composites that have been used in the photodegradation process were washed with distilled water, ethanol and dried in an oven for 1 hour at a temperature of 100 °C [28], [37]. The reduction in removal efficiency of NiO-NiFe$_2$O$_4$ composites after 3 cycles was only 2.24% (as shown in Fig. 11).
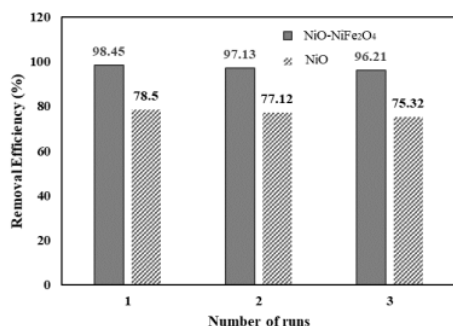

Fig. 11. The recyclability of NiO and NiO-NiFe$_2$O$_4$ composite (Congo red =50 mg/L, catalyst = 0.05 g, pH solution = 6, and irradiation time =120 min).

IV. CONCLUSION

A semiconductor NiO and a composite NiO-NiFe$_2$O$_4$ have been successfully synthesized and used for photocatalytic degradation of Congo red dye. The optimal photocatalytic degradation process was obtained at a pH of 6, the initial concentration of the dye congo red of 50 mg/L, and the irradiation duration using a visible light of 160 minutes. The removal efficiency of photocatalytic degradation of Congo red using the catalyst NiO-NiFe$_2$O$_4$ composite was 98.45 %, higher than that of 78.5% using NiO. It was proven that

doping NiFe$_2$O$_4$ on NiO increased the removal efficiency of photocatalytic degradation. Pseudo-first-order kinetics are suitable to describe the photocatalytic degradation of Congo red dye using either the photocatalyst NiO or NiO-NiFe$_2$O$_4$ composite. NiO-NiFe$_2$O$_4$ composite has high effectiveness of photodegradation. Even after 3 times reuse, it shows a large removal efficiency of 96.21%. The composite of NiO-NiFe$_2$O$_4$ has the potential to treat wastewater that contains dyes, especially Congo red.

CONFLICT OF INTEREST

The authors declare no conflict of interest.

AUTHOR CONTRIBUTIONS

Poedji Loekitowati Hariani, Muhammad Said, and Addy Rachmat did the laboratory work; Astri Nurmansyah and Ra Hoetary conducted data analysis. All authors participated in writing articles and approved the final version.

REFERENCES

[1] S. D. Khairnar and V. S. Shrvastava, "Facile synthesis of nickel oxide nanoparticles for the degradation of Methylene blue and Rhodamine B dye: A comparative study," *Journal of Taibah University for Science*, vol. 13, no. 1, pp. 1108-1118, 2019.

[2] R. S. Farias, H. L. B. Buargue, M. R. Cruz, L. M. F. Cardoso, T. A. Gondlm, and V. R. Paulo, "Adsorption og congo red dye from aqueous solution onto amino-functionalised silica gel," *Engenharia Sanitaria e Ambiental*, vol. 23, no. 6, pp. 1053-1060, 2018.

[3] K. Rehman, T. Shahzad, A. Sahar, S. Hussain, F. Mahmood, M. Siddique, M. A. Siddique, and M. I. Rashid, "Effect of reactive black 5 azo dye on soil processes related to C and N cycling," *Peer J*, vol. 6, 1-14, 2018.

[4] E. Pino, C. Calderon, F. Herrera, G. Cifuentes, and G. Arteaga, "Photocatalytic degradation of aqueous Rhodamine 6G using supported TiO$_2$ catalysts. A model for the removal of organic contaminants from aqueous samples," *Frontiers in Chemistry*, vol. 8, no. 365. pp. 1-12, 2020.

[5] H. Sachdeva and R. Saroj, "ZnO nanoparticles as an efficient, heterogeneous, reusable, and ecofriendly catalyst for four-component one-pot green synthesis of pyranopyrazole derivatives in water," *The Scientific World Journal*, vol. 2013, pp. 1-8, 2013.

[6] K. Bejtka, J. Zeng, A. Sacco, M. Castellino, S. Hernandez, M. A. Farkhondehfal, U. Savino, S. Ansaloni, C. Pirri, and A. Chiodoni," Chainlike mesoporous SnO$_2$ as a well-performing catalyst for electrochemical CO2 reduction," *Applied Energy Materials*, vol. 2, no. 5, pp. 3081-3091, 2019.

[7] M. Ramesh, M. P. C. Rao, S. Anandan, and H. Nagaraja, "Adsorption and photocatalytic properties of NiO nanoparticles synthesized via a thermal decomposition process," *Journal of Materials Research*, vol. 33, no. 5, pp. 601-610, 2018.

[8] A. J. Haider, R. Al-Anbari, H. M. Sami, and M. J. Haider, "Photocatalytic activity of nickel oxide," *Journal of Materials Research and Technology*, vol. 8, no. 3, pp. 2802-2808, 2019.

[9] F. Motahari, M. R. Mozdianfard, F. Soofivand, and M. S. Niasari, "NiO nanostructures: synthesis, characterization and photocatalyst application in dye wastewater treatment," *RSC Advances*, vol. 15, no. 4, pp. 27654-27660, 2014.

[10] Z. Qing, L. Haixia, L. Huali, L. Yu, Z. Huayong, and L. Tianduo, "Solvothermal synthesis and photocatalytic properties of NiO ultrathin nanosheets with porous structure," *Applied Surface Science*, vol. 328, pp. 525-530, 2015.

[11] K. Anandan and V. Rajendran, "Effects of Mn on the magnetic and optical properties and photocatalytic activities of NiO nanoparticles synthesized via the simple precipitation process," *Materials Science and Engineering: B*, vol. 199, pp. 48-56, 2015.

[12] I. Khosravi, M. Eftekhar," Characterization and evaluation catalytic efficiency of NiFe$_2$O$_4$ nano spinel in removal of reactive dye from aqueous solution," *Powder Technology*, vol. 250, pp. 147-153, 2013.

[13] N. M. Deraz, A. Alarifi, and S. A. Shaban, "Removal of sulfur from commercial kerosene using nanocrystalline NiFe2O4 based sorbents," *Journal of Saudi Chemical Society*, vol. 14, no. 4, pp. 357-362, 2010.

[14] K. S. Lin, A. K. Adhikari, C. Y. Wang, P. J. Hsu, and H. Y. Chan, "Synthesis and characterization of nickel and zink ferrite nanocatalysts for decomposition of CO2 greenhouse effect gas," *Journal of Nanoscience and Nanotechnology*, vol. 13, no. 4, pp. 2538-2548, 2013.

[15] R. Talebi, "Preparation of nickel ferrite nanoparticles via a new route and study of their photocatalytic properties," *Journal of Materials Science: Materials in Electronics*, vol. 28, pp. 4058–4063, 2017.

[16] H. Aliyan, R. Fazaeli, and R. Jalilian,"Fe$_3$O$_4$@mesoporous SBA-15: A magnetically recoverable catalyst for photodegradation of Malachite green," *Applied Surface Science*, vol. 276, pp. 147-153, 2013.

[17] A. Buthiyappan, A. R. A. Aziz, and W. M. A. W. Daud," Recent advances and prospects of catalytic advanced oxidation process in treating textile effluents," *Review in Chemical Engineering*, vol. 32, no. 1, pp. 147, 2015.

[18] E. Casbeer, V. K. Sharma, and X. Z. Li, "Synthesis and photocatalytic activity of ferrites under visible light: A review," *Separation and Purification Technology*, vol. 87, pp. 1-14, 2012.

[19] A. Ren, C. Liu, Y. Hong, W. Shi, S. Lin, and P. Li, "Enhanced visible-light-driven photocatalytic activity for antibiotic degradation using magnetic," *Chemical Engineering Journal*, vol. 258, pp. 301-308, 2014

[20] S. V. Bhosale, N. S. Kanhe, S. V. Bhoraskar, S. K. Bhat, R. N. Bulakhe, J. J. Shim, and V. L. Mathe, "Micro-structural analysis of NiFe2O4 nanoparticles synthesized by thermal plasma route and its suitability for BSA adsorption," *Journal of Materials Science: Materials in Medicine*, vol. 26, pp. 216–230, 2015.

[21] H. Y. Zhu, R. Jiang, S. H. Huang, J. Yao, F. Q. Fu, and J. B. Li, "Novel magnetic NiFe$_2$O$_4$/multi-walled carbon nanotubes hybrids: facile synthesis, characterization, and application to the treatment of dyeing wastewater," *Ceramic Internasional*, vol. 41, pp. 11625-11631, 2015.

[22] H. Y. Zhu, R. Jiang, Y. Q. Fu, R. R. Li, J. Yao, and S. T. Jiang, "Novel multifunctional NiFe$_2$O$_4$/ZnO hybrids for removal by adsorption, photocatalysis and magnetization separation," *Applied Surface Science*, vol. 369, pp. 1-10, 2016.

[23] L. Liu, N. Hu, Y. An, X. Du, X. Zhang, Y. Li, Y. Zeng, and Z. Cui, "Ag$_2$O and NiO decorated CuFe$_2$O$_4$ with enhanced photocatalytic performance to improve the degradation efficiency of methylene blue," *Materials*, vol. 13, pp. 1-12, 2020.

[24] Rahmayeni, S. Arief, Y. Stiadi, R. Rizal, and Zulhadjri, "Synthesis of magnetic nanoparticles of TiO2-NiFe2O4: characterization and photocatalitic activity on degradation of Rhodamin B," *Indonesian Journal of Chemistry*, vol. 12, no. 3, pp. 229-234, 2012.

[25] Rahmayeni, A. Alfina, Y. Stiadi, H. J. Lee, and Zulhadjri, "Green synthesis and characterization of ZnO-CoFe2O4 semiconductor photocatalysts Prepared using rambutan (Nephelium lappaceum L.) peel extract," *Materials Research*, vol. 22, no. 5, pp. 229-234, 2019.

[26] H. Y. Zhu, R. Jiang, Y. Q. Fu, R. R. Li, J. Yao, and S. T. Jiang," Novel multifunctional NiFe$_2$O$_4$/ZnO hybrids for dye removal by adsorption, photocatalysis and magnetic separation," *Applied Surface Science*, vol. 369, pp. 1-10, 2016.

[27] G. A. Babu, G. Ravi, M. Navaneethan, M. Arivanandhan, and Y. Hayakawa, "An ivestigation of flower shaped NiO nanostructures by microwave and hydrothermal route," *Journal of Materials Science: Materials in Electronics*, vol. 12, pp. 1-11, 2014.

[28] M. A. Sayed, M. M. Abo-Aly, A. A. A. Aziz, A. Hassan, and A. N. M. Salem, "A facile hydrothermal synthesis of novel CeO2/CdSe and CeO2/CdTe nanocomposites: spectroscopy investigations for economically feasible photocatalytic degradation of Congo red dye," *Inorganic Chemistry Communications*, vol. 130, pp. 1-11, 2021.

[29] M. Jain, M. Yadav, T. Kohout, M. Lahtinen, V. K. Garg, and M. Sillanpaa, "Development of iron oxide/activated carbon nanoparticle composite for the removal of Cr(VI), Cu(II) and Cd(II) ions from aqueous solution," *Water Resources and Industry*, vol. 20, pp. 54-74, 2018.

[30] H. Qiao, Z. Wei, L. Zhu, and X. Yan, "Preparation and characterization of NiO nanoparticles by anodic arc plasma method," *Journal of Nanomaterials*, vol. 2009, pp. 1-5, 2009.

[31] J. Saju and O. N. Balasundaram,"Optimization and characterization of NiO thin film prepared via NSP technique and its P-N juntion diode application," *Material Science Poland*, vol. 37, no. 3, pp. 1-9, 2019.

[32] P. L. Hariani, M. Said, A. Rachmat, F. Riyanti, H. C. Pratiwi, W. T. Rizki, "Preparation of NiFe$_2$O$_4$ nanoparticles by solution combustion methods as photocatalyst of Congo Red," *Bulletin of Chemical Reaction Engineering & Catalysis*, vol. 16, no. 3, pp. 481-490, 2021.

[33] P. Raizada, J. Kumari, P. Shandilya, and P. Singh, "Kinetics of photocatalytic mineralization of oxytetracycline and ampicillin using activated carbon supported ZnO/ZnWO," *Desalination and Water Treatment*, vol. 79, pp. 204-213, 2017.

[34] N. Ali, A. Said, F. Ali, F. Razig, Z. Ali, M. Bilal, L. Reinert, T. Begum, and H. M. N. Iqbal, "Photocatalytic degradation of Congo red dye from aqueous environment using cobalt ferrite nanostructure: Development, characterization, and photocatalytic Performance," *Water Air Soil Pollution*, vol. 231, no. 50, pp. 1-16, 2020.

[35] L. Curkovic, D. Ljubas, H. Juretic, "Photocatalytic decolorization kinetics of diazo Congo red aqueous solution by UV/TiO$_2$ nanoparticles," *Reaction Kinetics, Mechanisms and Catalysis*, vol. 99, pp. 201-208, 2010.

[36] U. O. Bhagwat, J. J. Wu, A. M. Asiri, S. Anandan," Sonochemical synthesis of Mg-TiO$_2$ nanoparticles for persistent Congo red dye degradation," *Journal of Photochemistry and Photobiology A: Chemistry*, vol. 346, pp. 559-569, 2017.

[37] A. S. Darwish, M. A. Sayed, and A. Shebl, "Cuttlefish bone stabilized Ag3VO4 nanocomposite and its Y2O3-decorated form: Waste-to-value development of efficiently ecofriendly visible-light-photoactive for dyeing, bacterial and larvae depollution of Egypt's wastewater," *Journal of Photochemistry & Photobiology A: Chemistry*, vol. 401, pp. 3-19, 2020.

Poedji Loekitowati Hariani was born in Madiun, East Java, Indonesia. She is a professor in chemistry at the Department of Chemistry, Faculty of Mathematics and Natural Sciences, Sriwijaya University, Palembang, Indonesia. She is also a researcher at the Research Center of Advanced Materials and Nanocomposite, Faculty of Mathematics and Natural Sciences, Sriwijaya University, Indonesia. His research is on materials applied to waste treatment, especially magnetic and composite materials for adsorption and photodegradation processes.

Comparison of the Photocatalytic Degradation of Congo Red Dye Using NiO and NiO-NiFe2O4 Composite

18% SIMILARITY INDEX

15% INTERNET SOURCES

16% PUBLICATIONS

5% STUDENT PAPERS

1 journal.gnest.org
Internet Source
3%

2 link.springer.com
Internet Source
2%

3 peerj.com
Internet Source
1%

4 Submitted to Al Al Bayt University
Student Paper
1%

5 irgu.unigoa.ac.in
Internet Source
1%

6 sciencetechindonesia.com
Internet Source
1%

7 Abolfazl Naseri, Mojtaba Goodarzi, Davood Ghanbari. "Green synthesis and characterization of magnetic and effective photocatalyst NiFe2O4–NiO nanocomposites", Journal of Materials Science: Materials in Electronics, 2017
Publication
1%

8   pubs.rsc.org
    Internet Source   1 %

9   K. Maniammal, G. Madhu, V. Biju.
    "Nanostructured mesoporous NiO as an
    efficient photocatalyst for degradation of
    methylene blue: Structure, properties and
    performance", Nano-Structures & Nano-
    Objects, 2018   1 %
    Publication

10 Rohit Jasrotia, Nisha Kumari, Rajesh Kumar,
    Mu. Naushad, Pooja Dhiman, Gaurav Sharma.
    "Photocatalytic degradation of environmental
    pollutant using nickel and cerium ions
    substituted Co0.6Zn0.4Fe2O4 nanoferrites",
    Earth Systems and Environment, 2021   1 %
    Publication

11 Pardeep Singh, Sonu, Pankaj Raizada, Anita
    Sudhaik, Pooja Shandilya, Pankaj Thakur,
    Shilpi Agarwal, Vinod Kumar Gupta.
    "Enhanced photocatalytic activity and stability
    of AgBr/BiOBr/graphene heterojunction for
    phenol degradation under visible light",
    Journal of Saudi Chemical Society, 2019   1 %
    Publication

12 www.jeeng.net
    Internet Source   1 %

13   Noor Zada, Idrees Khan, Tariq Shah, Tamanna Gul, Nasib Khan, Khalid Saeed. "Ag–Co oxides nanoparticles supported on carbon nanotubes as an effective catalyst for the photodegradation of Congo red dye in aqueous medium", Inorganic and Nano-Metal Chemistry, 2020
Publication   1 %

14   Submitted to UCSI University
Student Paper   1 %

15   Submitted to VIT University
Student Paper   1 %

16   Pooja Shandilya, Divya Mittal, Mahesh Kumar, Pankaj Raizada, Ahmad Hosseini-Bandegharaee, Adesh K. Saini, Pardeep Singh. "Fabrication of fluorine doped graphene and SmVO4 based dispersed and adsorptive photocatalyst for abatement of phenolic compounds from water and bacterial disinfection", Journal of Cleaner Production, 2018
Publication   1 %

17   jurnal.ugm.ac.id
Internet Source   1 %

18   rosap.ntl.bts.gov
Internet Source   1 %